from the arenethiol groups to the alkanethiolate ligands of a cluster such as $[Fe_4S_4(SEt)_4]^{2-}$.[63] We have also shown that cubane clusters are isolated in high yield from reactions employing the trianion of ligand **1** in Me_2SO solutions.[47] These results suggest that $(Me_2LS_3)^{3-}$ is predisposed to cluster capture in a manner similar to the protonated ligand.[64]

Interactions with Other Clusters. With the demonstration that ligands **1** and **2** bind essentially quantitatively to a cubane cluster, the question arises as to whether their flexibility is sufficient for them to bind as tridentates to clusters of other shapes. The only clusters currently available for such a test are the prismanes $[Fe_6S_6L_6]^{2-,3-}$ (**14**, L = halide, ArO^-).[65] Reaction of $[Fe_6S_6(OC_6H_4\text{-}p\text{-}Me)_6]^{3-}$ and 2 equiv of **1** in Me_2SO yielded one or more products whose ^1H NMR shifts are entirely consistent with the $[Fe_4S_4]^{2+}$ core.[2,13-15] The spectrum did not, however, correspond to $[Fe_4S_4(Me_2LS_3)(OC_6H_4\text{-}p\text{-}Me)]^{2-}$, which has been independently prepared by the reaction of cluster **4** and sodium cresolate.[13,66] The products have not been further identified. Additionally, reaction of $[Fe_6S_6Cl_6]^{3-}$ with 1 or 2 equiv of **1** (in the presence of 3 or 6 equiv of Et_3N) in acetonitrile gave **4** as the only product detectable by ^1H NMR.

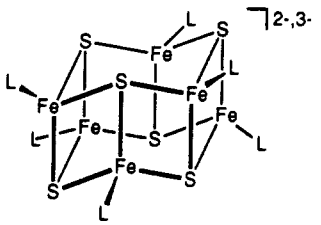

14

Only cubane-type products have been identified from the reactions of prismanes and ligand **1**. The prismane cluster presents two faces to an attacking ligand: an Fe_3S_3 ring whose Cl···Cl separations are 7.3 Å and two fused Fe_2S_2 rhombs whose Cl···Cl separations are two at 5.5 Å and one at 7.3 Å. These may be too demanding of ligand flexibility, which in four $[Fe_4Q_4]^{2+}$ structures (**4**, **5**) is required to span S···S distances of 6.42-6.67 Å.

Acknowledgment. This research was supported by NIH Grant GM 28856. X-ray equipment was obtained through NIH Grant 1 S10 RR 02247. We thank Professor M. Karplus and Dr. J. R. Smith for useful discussions and Dr. G. Henkel for permission to quote structural results prior to publication.

Supplementary Material Available: Crystallographic data for $(Ph_4P)_2[Fe_4Se_4(Me_2LS_3)Cl]\cdot 2DMF$, including tables of intensity collection and structure refinement parameters, temperature factors, interatomic distances and angles, and positional parameters including hydrogen atoms, a table of chemical shifts of compounds in Table VII and others used in establishing assignments, and plots of tilt angle distributions and maximum vs intermediate cant values for configurations of **1** and **3** from molecular dynamics calculations (19 pages); a table of structure factors (49 pages). Ordering information is given on any current masthead page.

(63) Dukes, G. R.; Holm, R. H. *J. Am. Chem. Soc.* **1975**, *97*, 528.

(64) While we have not attempted to evaluate the shielding of 2-H in $(Me_2LS_3)^{3-}$ with the use of anionic reference compounds, its chemical shift (6.49 ppm in Me_2SO) is very close to that of **1** (6.45 ppm in $CDCl_3$) at 297 K. Other chemical shifts of the trianion are as follows: δ 1.82 (4-Me), 2.05 (6-Me), 2.24 (4'-Me), 6.79 (5-H), 6.80 (3'-H), 7.05 (2'-H). Ligand **1** is not soluble in Me_2SO, so that a direct comparison of shifts in the same solvent is not available.

(65) (a) Coucouvanis, D.; Kanatzidis, M. G.; Dunham, W. R.; Hagen, W. R. *J. Am. Chem. Soc.* **1984**, *106*, 7998. (b) Kanatzidis, M. G.; Hagen, W. R.; Dunham, W. R.; Lester, R. K.; Coucouvanis, D. *J. Am. Chem. Soc.* **1985**, *107*, 953. (c) Kanatzidis, M. G.; Salifoglou, A.; Coucouvanis, D. *Inorg. Chem.* **1986**, *25*, 2460.

(66) Chemical shifts: reaction product, δ 8.10 (5-H), 3.83 (6-Me), 3.60 (4-Me) (main signals of the arms); authentic $[Fe_4S_4(Me_2LS_3)(OC_6H_4\text{-}p\text{-}Me)]^{2-}$, δ 8.77 (m-H), 8.23 (5-H), 4.66 (p-Me), 3.95 (6-Me), 3.71 (4-Me).

Contribution from the Department of Chemistry,
The University of North Carolina, Chapel Hill, North Carolina 27599-3290

Synthesis, Structure, and Redox Properties of the Triaqua(tris(1-pyrazolyl)methane)ruthenium(II) Cation

Antoni Llobet,[1a] Derek J. Hodgson,[1b] and Thomas J. Meyer*[,1c]

Received August 15, 1989

The synthesis of the salt $[(tpm)Ru(H_2O)_3](p\text{-}CH_3C_6H_4SO_3)_2\cdot 1.5H_2O$, where tpm is the terdentate facial ligand tris(1-pyrazolyl)methane, is described. The salt was prepared as a possible precursor to a structurally stabilized but reactive *cis*-dioxoruthenium(VI) oxidant. The crystal structure of the salt has been determined from three-dimensional X-ray data. It crystallizes in the triclinic space group $P\bar{1}$ with two formula units in a cell of dimensions a = 10.780 (5) Å, b = 11.122 (8) Å, c = 14.489 (4) Å, α = 74.60 (5)°, β = 67.23 (4)°, and γ = 87.41 (5)°. The structure has been refined to a final value of R = 0.031 based on the intensities of 3390 reflections. The crystal structure proves that the complex is the *fac* isomer in which the terdentate ligand occupies three sites on one face of the coordination octahedron and the three water molecules occupy the opposite face. Electrochemical studies at activated glassy-carbon electrodes show the appearance of waves for Ru(III/II), Ru(IV/III), and Ru(V/IV) couples. Oxidation past Ru(IV) leads to an opening of one of the chelating arms of the tpm ligand and formation of a *trans*-dioxo complex of Ru(VI).

Introduction

For complexes of osmium and ruthenium a diverse higher oxidation state chemistry exists based on metal-oxo formation.[2-5] Characteristically, the higher oxidation states can be reached by sequential oxidation and proton loss from lower oxidation state

(1) (a) Fulbright "La Caixa" Fellow, Barcelona, Spain. Permanent address: Department de Quimica (Area 10), Universitat Autonoma de Barcelona, 08193 Bellaterra, Barcelona, Spain. (b) Department of Chemistry, University of Wyoming. (c) Department of Chemistry, The University of North Carolina.

(2) (a) Moyer, B. A.; Meyer, T. J. *J. Am. Chem. Soc.* **1978**, *100*, 3601. (b) Moyer, B. A.; Meyer, T. J. *Inorg. Chem.* **1981**, *20*, 436. (c) Pipes, D. W.; Meyer, T. J. *J. Am. Chem. Soc.* **1984**, *106*, 7653. (d) Gilbert, J. A.; Eggleston, D. S.; Murphy, W. R., Jr.; Geselowitz, D. A.; Gersten, S. W.; Hodgson, D. J.; Meyer, T. J. *J. Am. Chem. Soc.* **1985**, *107*, 3855. (e) Gilbert, J. A.; Geselowitz, D. A.; Meyer, T. J. *J. Am. Chem. Soc.* **1986**, *108*, 1493. (f) Pipes, D. W.; Meyer, T. J. *Inorg. Chem.* **1986**, *25*, 4042. (g) Doppelt, P.; Meyer, T. J. *Inorg. Chem.* **1987**, *26*, 2027.

0020-1669/90/1329-3760$02.50/0

aqua complexes of Ru(II) or Os(II). An example is shown in eq 1,[2a,b] where bpy is 2,2'-bipyridine and py is pyridine. The ready

$$[(bpy)_2(py)Ru^{II}(H_2O)]^{2+} \underset{+e,\,+H^+}{\overset{-e,\,-H^+}{\rightleftharpoons}} [(bpy)_2(py)Ru^{III}(OH)]^{2+} \underset{+e,\,+H^+}{\overset{-e,\,-H^+}{\rightleftharpoons}} [(bpy)_2(py)Ru^{IV}(O)]^{2+} \quad (1)$$

accessibility to the higher oxidation states has led to the development of a versatile stoichiometric and/or catalytic oxidation chemistry toward a variety of inorganic and organic substrates.[4b,d,5a,b,6,7]

Among the polypyridyl examples are *cis*- and *trans*-$[(B)_2M^{II}(H_2O)_2]^{2+}$ (B = bpy, 2,9-dimethyl-1,10-phenanthroline, 6,6'-dichloro-2,2'-bipyridine; M = Ru, Os) where chemical or electrochemical oxidation leads to *cis*- or *trans*-$[(B)_2M^{VI}(O)_2]^{2+}$.[8] In terms of chemical reactivity, the cis complexes with their *cis*-dioxo structures are of special interest. They are potential electrocatalysts that, conceivably, could mimic the reactivity properties of such oxidants as OsO_4 or RuO_4.[9] They have implied reactivities as four-electron oxidants in pathways that could utilize both *O* atoms.[8e-g,10] Compared to the trans complexes, where there is a considerable electronic stabilization of the d^2 electronic configuration of M(VI) by the *trans*-dioxo group, the cis complexes are considerably stronger oxidants thermodynamically.[8a,f]

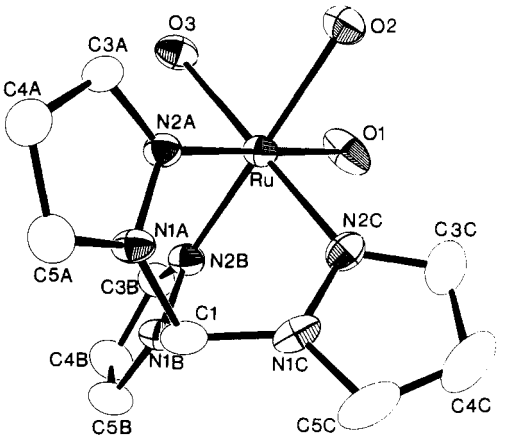

Figure 1. View of the cation. Thermal ellipsoids are drawn at the 40% probability level. Carbon atoms are shown as open ellipsoids, and hydrogen atoms are omitted for clarity.

A second point of interest in a reactivity sense arises from the potential of the Ru(VI)/Ru(II) *cis*-dioxo couple (eq 2). The

$$cis\text{-}[(bpy)_2Ru^{VI}(O)_2]^{2+} + 4e + 4H^+ \rightarrow cis\text{-}[(bpy)_2Ru^{II}(H_2O)_2]^{2+} \quad (2)$$

potential of this couple is 1.26 V vs NHE at pH = 0,[8f] showing that, at least in a thermodynamic sense, the *cis*-dioxoruthenium(VI) complex is capable of oxidizing water to dioxygen at a single site, eq 3.

$$cis\text{-}[(bpy)_2Ru^{VI}(O)_2]^{2+} + 2H_2O \rightarrow cis\text{-}[(bpy)_2Ru^{II}(H_2O)_2]^{2+} + O_2 \quad (3)$$

$$\Delta G^{\circ\prime} = -0.12 \text{ eV}$$

Attempts to investigate and exploit the oxidative properties of *cis*-$[(bpy)_2Ru^{VI}(O)_2]^{2+}$ and related complexes have been inhibited by the rapid loss of a bpy ligand in aqueous solution.[8f] The driving force for the ligand loss chemistry is the electronic stabilization associated with the formation of the *trans*-dioxo group in the product, eq 4.

$$cis\text{-}[(bpy)_2Ru^{VI}(O)_2]^{2+} + 2H_2O \rightarrow trans,cis\text{-}[(bpy)Ru^{VI}(O)_2(OH)_2] + bpyH^+ + H^+ \quad (4)$$

The appearance of the ligand loss chemistry prompted us to search for new ligand systems that might stabilize the *cis*-dioxo structure. One approach to this problem has been described by Che et al. and involves the substitution of relatively bulky chloro groups for H at the 6- and 6'-positions of the bpy ligand.[7h,8a] The approach that we describe here was to turn to an ancillary ligand which might enforce the *cis*-dioxo geometry at the metal as a way of avoiding ligand loss and *trans*-dioxo formation. We chose the facial terdentate ligand tris(1-pyrazolyl)methane (tpm).[11] The hope was that the facial geometry required by the ligand would prevent *trans*-dioxo formation in the higher oxidation states. In addition, this ligand offers the possible advantage of studying a complex in which there are three water molecules bound to ruthenium in an enforced facial geometry. Here we report the synthesis and crystal structure of the triaqua complex [(tpm)-

(3) (a) Che, C.-M.; Tang, W. T.; Poon, C. K. *J. Chem. Soc., Chem. Commun.* **1984**, 641. (b) Che, C.-M.; Wong, K. Y.; Poon, C. K. *Inorg. Chem.* **1985**, *24*, 1797. (c) Che, C.-M.; Wong, K. Y.; Mak, T. C. W. *J. Chem. Soc., Chem. Commun.* **1985**, 546. (d) Che, C.-M.; Wong, K. Y.; Leung, W. H.; Poon, C. K. *Inorg. Chem.* **1986**, *25*, 345. (e) Che, C.-M.; Wong, K. Y. *J. Chem. Soc., Chem. Commun.* **1986**, 229. (f) Che, C.-M.; Cheng, W. K. *J. Am. Chem. Soc.* **1986**, *108*, 4644. (g) Che, C.-M.; Cheng, W. K. *J. Chem. Soc., Chem. Commun.* **1986**, 1519. (h) Che, C.-M.; Lai, T. F.; Wong, K. Y. *Inorg. Chem.* **1987**, *26*, 2289. (i) Che, C.-M.; Cheng, W. K.; Mak, T. C. W. *Inorg. Chem.* **1988**, *27*, 250. (j) Che, C.-M.; Cheng, W. K.; Tang, W. T. *Inorg. Chem.* **1988**, *27*, 2801.

(4) (a) Groves, J. T.; Quinn, R. *Inorg. Chem.* **1984**, *23*, 3844. (b) Groves, J. T.; Quinn, R. *J. Am. Chem. Soc.* **1985**, *107*, 5790. (c) Groves, J. T.; Ahn, K. H. *Inorg. Chem.* **1987**, *26*, 3831. (d) Groves, J. T.; Ahn, K. H.; Quinn, R. *J. Am. Chem. Soc.* **1988**, *110*, 4217.

(5) (a) Leising, R. A.; Takeuchi, K. J. *Inorg. Chem.* **1987**, *26*, 4391. (b) Marmion, M. E.; Takeuchi, K. J. *J. Chem. Soc., Chem. Commun.* **1987**, 1396. (c) Marmion, M. E.; Takeuchi, K. J. *J. Am. Chem. Soc.* **1988**, *110*, 1472.

(6) (a) Moyer, B. A.; Meyer, T. J. *J. Am. Chem. Soc.* **1979**, *101*, 1326. (b) Moyer, B. A.; Thompson, M. S.; Meyer, T. J. *J. Am. Chem. Soc.* **1980**, *102*, 2310. (c) Moyer, B. A.; Sipe, B. K.; Meyer, T. J. *Inorg. Chem.* **1981**, *20*, 1475. (d) Binstead, R. A.; Moyer, B. A.; Samuels, G. J.; Meyer, T. J. *J. Am. Chem. Soc.* **1981**, *103*, 2897. (e) Thompson, M. S.; Meyer, T. J. *J. Am. Chem. Soc.* **1982**, *104*, 4106. (f) Thompson, M. S.; Meyer, T. J. *J. Am. Chem. Soc.* **1982**, *104*, 5070. (g) Gersten, S. W.; Samuels, G. J.; Meyer, T. J. *J. Am. Chem. Soc.* **1982**, *104*, 4029. (h) Thompson, M. S.; DeGiovani, W. F.; Moyer, B. A.; Meyer, T. J. *J. Org. Chem.* **1984**, *49*, 4972. (i) Meyer, T. J. *J. Electrochem. Soc.* **1984**, *131*, 221C. (j) Takeuchi, K. J.; Thompson, M. S.; Pipes, D. W.; Meyer, T. J. *Inorg. Chem.* **1984**, *23*, 1845. (k) Kutner, W.; Meyer, T. J.; Murray, R. W. *J. Electroanal. Chem. Interfacial Electrochem.* **1985**, *375*, 195. (l) Vining, W. J.; Meyer, T. J. *Inorg. Chem.* **1986**, *25*, 2023. (m) Dobson, J. C.; Seok, W. K.; Meyer, T. J. *Inorg. Chem.* **1986**, *25*, 1514. (n) Kutner, W.; Gilbert, J. A.; Tomaszewski, A.; Meyer, T. J.; Murray, R. W. *J. Electroanal. Chem. Interfacial Electrochem.* **1986**, *205*, 185. (o) Roecker, L.; Meyer, T. J. *J. Am. Chem. Soc.* **1986**, *108*, 4066. (p) Roecker, L.; Dobson, J. C.; Vining, W. J.; Meyer, T. J. *Inorg. Chem.* **1987**, *26*, 779. (q) Gilbert, J.; Roecker, L.; Meyer, T. J. *Inorg. Chem.* **1987**, *26*, 1126. (r) Roecker, L.; Meyer, T. J. *J. Am. Chem. Soc.* **1987**, *109*, 746. (s) Binstead, R. A.; Meyer, T. J. *J. Am. Chem. Soc.* **1987**, *109*, 3287. (t) Seok, W. K.; Dobson, J. C.; Meyer, T. J. *Inorg. Chem.* **1988**, *27*, 3. (u) Seok, W. K.; Meyer, T. J. *J. Am. Chem. Soc.* **1988**, *110*, 7358.

(7) (a) Che, C.-M.; Lai, T. F.; Chung, W. C.; Schaefer, W. P.; Gray, H. B. *Inorg. Chem.* **1987**, *26*, 3907. (b) Che, C.-M.; Leung, W. H. *J. Chem. Soc., Chem. Commun.* **1987**, 1376. (c) Wong, K. W.; Che, C.-M.; Anson, F. C. *Inorg. Chem.* **1987**, *26*, 737. (d) Lau, T. C.; Kochi, J. K. *J. Chem. Soc., Chem. Commun.* **1987**, 798. (e) Yam, V. W. W.; Che, C.-M.; Tang, W. T. *J. Chem. Soc., Chem. Commun.* **1988**, 100. (f) Che, C.-M.; Lee, W.-O. *J. Chem. Soc., Chem. Commun.* **1988**, 881. (g) Che, C. M.; Tang, W. T.; Wong, W. T.; Lai, T. F. *J. Am. Chem. Soc.* **1989**, *111*, 9048. (h) Leung, W. H.; Che, C. M. *J. Am. Chem. Soc.* **1989**, *111*, 8812.

(8) (a) Che, C.-M.; Leung, W.-H. *J. Chem. Soc., Chem. Commun.* **1987**, 1376. (b) Bailey, C. L.; Drago, R. S. *J. Chem. Soc., Chem. Commun.* **1987**, 1377. (c) Collin, J. P.; Sauvage, J. P. *Inorg. Chem.* **1986**, *25*, 135. (d) Takeuchi, K. J.; Samuels, J. G.; Gersten, S. W.; Gilbert, J. A.; Meyer, T. J. *Inorg. Chem.* **1983**, *22*, 1407. (e) Dobson, J. C.; Takeuchi, K. J.; Pipes, D. W.; Geselowitz, D. A.; Meyer, T. J. *Inorg. Chem.* **1986**, *25*, 2357. (f) Dobson, J. C.; Meyer, T. J. *Inorg. Chem.* **1988**, *27*, 3283. (g) Dobson, J. C.; Meyer, T. J. *Inorg. Chem.* **1989**, *28*, 2013.

(9) Cotton, F. A.; Wilkinson, G. *Advanced Inorganic Chemistry*, 5th ed.; J. Wiley and Sons: New York, 1988; pp 880–884.

(10) Nijs, F.; Cruz, M.; Fripiat, J. J.; Van Damme, H. *Nouv. J. Chim.* **1982**, *6*, 551.

(11) Hückel, W.; Bretschneider, H. *Ber. Chem.* **1937**, *9*, 2024.

$Ru(H_2O)_3]^{2+}$, its spectral properties, and its oxidation chemistry.

Experimental Section

Materials. All reagents were ACS grade and were used without further purification. Water was purified by a Millipure system. Elemental analysis were performed by Galbraith Laboratories, Knoxville, TN.

Preparations. [(tpm)Ru(μ-O)(μ-O_2P(O)(OH))$_2$Ru(tpm)]·5.5H_2O (**2**) was prepared as previously described.[12d]

[(tpm)Ru(H_2O)$_3$](p-$CH_3C_6H_4SO_3$)$_2$·1.5H_2O (1). A 200-mg sample of **2** was added to a 0.1 M *p*-toluenesulfonic acid solution that had been previously deaerated by N_2 bubbling. Zinc amalgam (5 g) was added, and the resulting mixture was stirred magnetically under argon until the solution turned pale yellow. The remaining solid was filtered off and the volume of the filtrate reduced to ~10 mL at low pressure. Upon cooling of the solution, light yellow crystals appeared, which were filtered in a Büchner funnel, washed with a small amount of cold water, and dried under vacuum. Yield: 238 mg, 76%. Anal. Calcd for $C_{24}H_{33}O_{10.5}N_6S_2Ru$: C, 39.02; H, 4.47; N, 11.38. Found: C, 39.22; H, 4.45; N, 11.38. ^{1}H NMR (D_2O): δ 8.2 (d, 3, J_{54} = 2.7 Hz, H(5)), 7.8 (d, 3, J_{34} = 1.9 Hz, H(3)), 7.5 (d, 4, J_{76} = 7.0 Hz, H(7)), 7.15 (d, 4, H(6)), 6.4 (doublet of doublets, 3, H(4)), 2.2 (s, 6, CH_3).

The ^{1}H NMR labels for the hydrogen atoms of the tpm ligand are keyed to the structure of the cation shown in Figure 1. The hydrogen atoms have been labeled in accordance with the numbering scheme for the corresponding carbon atoms to which they are bound. For example, hydrogen atoms H(5) include the hydrogen atoms bonded to carbon atoms, C(5A), C(5B), and C(5C) (see Figure 1). For the *p*-toluenesulfonate anion, the aromatic ring hydrogen atoms have been labeled H(6) and H(7). The label H(6) stands for the two equivalent hydrogen atoms that are proximal to the methyl group, while H(7) represents the two equivalent hydrogen atoms nearest to the sulfur atom.

Measurements. Cyclic voltammetric measurements were carried out by using a PAR Model 173 potentiostat/galvanostat or a PAR 264A polarographic analyzer. Coulometric measurements were made by using a PAR Model 179 digital coulometer. The cyclic voltammetric measurements utilized a Teflon-sheathed glassy-carbon disk (1.5-mm radius) as a working electrode, a platinum wire as the auxiliary electrode, and a saturated sodium chloride calomel reference electrode (SSCE) in a one-comparement cell. The glassy-carbon electrodes were activated in a specific, prescribed way.[13] The treatment involved maintaining the electrode at +1.8 V, for 30 s, and then holding the electrode at −0.2 V, for 15 s. This ritual was repeated three times in a 0.1 M sulfuric acid solution with a freshly polished glassy-carbon electrode. Electrodes treated in this way gave cyclic voltammetric waves in some pH regions that could not be observed when untreated glassy-carbon electrodes were used. Polishing the surface again with diamond paste restored the electrode to its initial, inactive form. The concentration of the complexes was approximately 1 mM, and unless explicitly specified the scan rate was 100 mV/s. A Tektronix 7623A oscilloscope was used as a recorder when the scan rates were higher than 200 mV/s. The pH measurements were made with a Radiometer pHM62 pH meter. In aqueous solutions the pH was adjusted from 0–2 with either perchloric or *p*-toluenesulfonic acid. Sodium perchlorate or sodium *p*-toluenesulfonate, respectively, were added to keep a minimum ionic strength of 0.1 M. From pH = 2–9, 0.1 M phosphate buffers were used, and from pH = 9–12, a 0.1 M borate buffer was used. Dilute NaOH, CO_2-free solutions were used to reach pH = 12–13 with sodium perchlorate added as electrolyte. All $E_{1/2}$ values reported in this work were estimated from cyclic voltammetry as the average of the oxidative and reductive peak potentials $(E_{p,a} + E_{p,c})/2$. UV–visible spectra were recorded by using a Hewlett-Packard Model 8451A UV-vis diode-array spectrophotometer with 1-cm quartz cells. The ^{1}H NMR spectra were recorded on an IBM AC-200 spectrometer.

X-ray Data Collection. Cell constants, obtained at 293 K from a least-squares analysis of the angular settings for 25 reflections on an Enraf-Nonius CAD-4 diffractometer equipped with a Mo tube and a Zr filter [λ(Kα1) = 0.709 26 Å, λ(Kα2) = 0.713 54 Å], were a = 10.780 (5) Å, b = 11.122 (8) Å, c = 14.489 (4) Å, α = 74.60 (5)°, β = 67.23 (4)°, and γ = 87.41 (5)°. Intensity data were collected on the same diffractometer by using Mo Kα radiation out to a maximum of 2θ(Mo) = 45°; a total of 4017 unique reflections were collected. A weighting scheme of the type described by Ibers and co-workers[14] was employed. The weighting factor p was set at 0.02. Data were corrected for Lorentz–polarization effects and for absorption, the transmission factors falling in the range 0.88–0.999 with an average value of 0.96. Of the 4017 data, only the 3390 intensities with $I > 3\sigma(I)$ were considered to be observed. They were used in the subsequent analysis. Crystallographic data are provided in Table I.

Table I. Crystallographic and Data Collection Parameters

formula	$RuC_{24}H_{30}N_6O_9S_2$·1.5H_2O	T, °C	21
a, Å	10.780 (5)	D_c, g cm^{-3}	1.592
b, Å	11.122 (8)	fw	738.79
c, Å	14.489 (4)	λ, Å	0.709 26
α, deg	74.60 (5)	space group	$P\bar{1}$ (No. 2)
β, deg	67.23 (4)	μ, cm^{-1}	6.89
γ, deg	87.41 (5)	max transm	0.999
V, Å^3	1541 (2)	min transm	0.88
Z	2	av transm	0.96
NO(tot)[a]	4017	data range	$2 < 2\theta < 45°$
NO(obs)	3390 [$I > 3\sigma(I)$]	data collcd	$\pm h, \pm k, \pm l$
radiation	Mo Kα	$R(F_o)$	0.031
		R_w	0.038

[a] NO = number of observations.

Table II. Atomic Positional Parameters in the Salt [(tpm)Ru(H_2O)$_3$](p-$CH_3C_6H_4SO_3$)$_2$·1.5H_2O

atom	x	y	z
Ru	0.22834 (3)	0.23794 (3)	0.07374 (2)
S(1)	0.0346 (1)	0.2459 (1)	0.82608 (7)
S(2)	0.2923 (1)	0.8446 (1)	0.69788 (8)
O(1)	0.1285 (3)	0.1069 (3)	0.0372 (2)
O(2)	0.2364 (2)	0.3742 (2)	−0.0644 (2)
O(3)	0.0394 (2)	0.3024 (2)	0.1542 (2)
OW(1)	0.1244 (3)	0.5978 (2)	0.9541 (2)
O(11)	−0.0340 (4)	0.3497 (3)	0.8575 (2)
O(12)	−0.0440 (5)	0.1340 (4)	0.8880 (3)
O(13)	0.1639 (3)	0.2446 (5)	0.8249 (2)
O(21)	0.3045 (3)	0.7649 (3)	0.7914 (2)
O(22)	0.1542 (3)	0.8755 (3)	0.7175 (2)
O(23)	0.3866 (3)	0.9522 (3)	0.6513 (2)
O(W2)	0.315 (2)	0.033 (2)	0.821 (1)
N(1A)	0.4239 (3)	0.3232 (3)	0.1398 (2)
N(2A)	0.3206 (3)	0.3608 (3)	0.1098 (2)
N(1B)	0.3466 (3)	0.1104 (3)	0.2194 (2)
N(2B)	0.2298 (3)	0.1126 (3)	0.2036 (2)
N(1C)	0.5023 (3)	0.1740 (3)	0.0441 (2)
N(2C)	0.4118 (3)	0.1848 (3)	−0.0021 (2)
C(1)	0.4605 (3)	0.1956 (3)	0.1446 (3)
C(3A)	0.3096 (4)	0.4799 (3)	0.1126 (3)
C(4A)	0.4050 (4)	0.5168 (3)	0.1437 (3)
C(5A)	0.4766 (4)	0.4157 (3)	0.1607 (3)
C(3B)	0.1457 (4)	0.0277 (4)	0.2843 (3)
C(4B)	0.2071 (4)	−0.0276 (4)	0.3518 (3)
C(5B)	0.3340 (4)	0.0259 (4)	0.3098 (3)
C(3C)	0.4809 (5)	0.1636 (4)	−0.0941 (3)
C(4C)	0.6131 (5)	0.1405 (4)	−0.1065 (4)
C(5C)	0.6244 (4)	0.1482 (4)	−0.0184 (4)
C(1P1)	0.0504 (4)	0.2619 (3)	0.6981 (3)
C(2P1)	0.1504 (4)	0.2045 (4)	0.6345 (3)
C(3P1)	0.1623 (5)	0.2179 (4)	0.5335 (3)
C(4P1)	0.0755 (5)	0.2862 (4)	0.4954 (3)
C(5P1)	−0.0266 (4)	0.3405 (4)	0.5610 (3)
C(6P1)	−0.0392 (4)	0.3285 (4)	0.6617 (3)
C(7P1)	0.0904 (6)	0.3037 (6)	0.3839 (3)
C(1P2)	0.3336 (4)	0.7532 (4)	0.6079 (3)
C(2P2)	0.4311 (4)	0.7963 (4)	0.5095 (3)
C(3P2)	0.4567 (5)	0.7271 (5)	0.4387 (4)
C(4P2)	0.3867 (5)	0.6143 (5)	0.4640 (4)
C(5P2)	0.2905 (5)	0.5717 (5)	0.5651 (4)
C(6P2)	0.2634 (5)	0.6396 (5)	0.6361 (4)
C(7P2)	0.4123 (6)	0.5421 (6)	0.3866 (4)

Solution and Refinement of the Structure. The location of the ruthenium atom was determined from examination of a Patterson function, and the positions of all other atoms were located from subsequent difference Fourier maps. The hydrogen atoms in the structure were all

(12) (a) Llobet, A.; Doppelt, P.; Meyer, T. J. *Inorg. Chem.* **1988**, *27*, 514. (b) Barqawi, K.; Llobet, A.; Meyer, T. J. *J. Am. Chem. Soc.* **1988**, *110*, 7751. (c) Llobet, A.; Meyer, T. J. Unpublished work. (d) Llobet, A.; Curry, M. E.; Evans, H. T.; Meyer, T. J. *Inorg. Chem.* **1989**, *28*, 3131.
(13) (a) Diamantis, A. A.; Murphy, W. R.; Linton, R. W.; Meyer, T. J. *Inorg. Chem.* **1984**, *24*, 3230. (b) Cabaniss, G. E.; Diamantis, A. A.; Murphy, W. R., Jr.; Linton, R. W.; Meyer, T. J. *J. Am. Chem. Soc.* **1985**, *107*, 1845.
(14) Corfield, P. W.; Doedens, R. J.; Ibers, J. A. *Inorg. Chem.* **1967**, *6*, 197.

Table III. Bond Lengths (Å) in [(tpm)Ru(H2O)3](p-CH3C6H4SO3)2·1.5H2O

	Cation		
Ru-N(2A)	2.008 (2)	C(3A)-C(4A)	1.387 (3)
Ru-N(2B)	2.028 (2)	C(4A)-C(5A)	1.357 (3)
Ru-N(2C)	2.006 (2)	N(1B)-N(2B)	1.362 (2)
Ru-O(1)	2.134 (1)	N(1B)-C(5B)	1.355 (3)
Ru-O(2)	2.139 (1)	N(2B)-C(3B)	1.323 (3)
Ru-O(3)	2.121 (1)	C(3B)-C(4B)	1.386 (3)
C(1)-N(1A)	1.447 (3)	C(4B)-C(5B)	1.354 (4)
C(1)-N(1B)	1.453 (3)	N(1C)-N(2C)	1.366 (3)
C(1)-N(1C)	1.431 (3)	N(1C)-C(5C)	1.348 (3)
N(1A)-N(2A)	1.357 (2)	N(2C)-C(3C)	1.331 (3)
N(1A)-C(5A)	1.350 (3)	C(3C)-C(4C)	1.386 (4)
N(2A)-C(3A)	1.335 (3)	C(4C)-C(5C)	1.353 (4)
	Anions		
S(1)-O(11)	1.424 (2)	C(3P1)-C(4P1)	1.368 (4)
S(1)-O(12)	1.409 (2)	C(4P1)-C(5P1)	1.384 (4)
S(1)-O(13)	1.387 (2)	C(4P1)-C(7P1)	1.520 (4)
S(1)-C(1P1)	1.756 (2)	C(5P1)-C(6P1)	1.384 (4)
S(2)-O(21)	1.459 (2)	C(1P2)-C(2P2)	1.375 (4)
S(2)-O(22)	1.448 (1)	C(1P2)-C(6P2)	1.382 (4)
S(2)-O(23)	1.439 (2)	C(2P2)-C(3P2)	1.379 (4)
S(2)-C(1P2)	1.773 (3)	C(3P2)-C(4P2)	1.380 (5)
C(1P1)-C(2P1)	1.379 (4)	C(4P2)-C(5P2)	1.395 (5)
C(1P1)-C(6P1)	1.372 (3)	C(4P2)-C(7P2)	1.483 (5)
C(2P1)-C(3P1)	1.385 (4)	C(5P2)-C(6P2)	1.370 (4)

located in difference maps with the exception of those on water molecule OW(2), which has an occupancy factor of 50% since this position corresponds to $^1/_2$ of a water molecule, the crystals having 1.5 H_2O per ruthenium. The final refinement involved isotropic refinement of this half-water oxygen atom, anisotropic refinement of all other non-hydrogen atoms (43 atoms), but no refinement of hydrogen atom parameters. Hydrogen atom isotropic thermal parameters were set to 1.5 Å^2 greater than those of the atom to which they are attached. The final values of the standard agreement factors R_1 and R_2 were 0.031 and 0.038, respectively. A final difference Fourier was featureless, with no peak higher than 0.24 e A^{-3}. In the final least-squares cycle, no parameters experienced a shift of more than 0.12σ, which was taken as evidence of convergence. Positional parameters are presented in Table II; listing of hydrogen atom positional parameters, anisotropic thermal parameters, and observed and calculated structure amplitudes are available as supplementary material.

Results

The tpm-based synthetic chemistry that was utilized here has its origins in previous work in this area.[15] It was developed in the preparation of the complexes $[(tpm)(4,4'\text{-}(X)_2\text{-bpy})Ru(L)]^{n+}$ (X = CH_3, Ph, NH_2, $COOC_2H_5$; L = Cl^- (n = 1); L = H_2O, O^{2-}, pyridine (n = 2))[12a-c] and in the preparation of a series of tris-(μ-oxo)-bridged dinuclear complexes such as $[(tpm)Ru^{III}(\mu\text{-}O)(\mu\text{-}O_2P(O)(OH))_2Ru^{III}(tpm)]$ (**2**).[12d]

Reduction by zinc amalgam of an acidic, blue aqueous solution containing the triply bridged complex [(μ-oxo)bis(μ-hydrogen phosphato)bis(tris(1-pyrazolyl)methane)diruthenium(III)] (**2**) leads to a yellow solution. The results of UV-visible spectroscopic studies show that the reduction produces the triaqua monomer $[(tpm)Ru(H_2O)_3]^{2+}$ (cation of **1**), quantitatively (reaction 5).

$$[(tpm)Ru^{III}(\mu\text{-}O)(\mu\text{-}O_2P(O)(OH))_2Ru^{III}(tpm)] + Zn(Hg) + 2H^+ \rightarrow 2[(tpm)Ru^{II}(H_2O)_3]^{2+} + Zn^{2+} + 2H_2PO_4^- \quad (5)$$

Description of the Structure. The structure of the salt of the triaqua complex consists of the complex cations, *p*-toluenesulfonate anions, and water molecules, which are linked together by hydrogen bonds. A view of the cation is shown in Figure 1, and the bond lengths and angles in the structure are listed in Tables III and IV, respectively. The geometry at ruthenium is approximately octahedral, the ligating atoms being the three N(2) atoms of the pyrazole moieties and three oxygen atoms of the water molecules. The isomer observed here is the *fac* isomer, in which each nitrogen atom is trans to an oxygen atom, as expected due to the constraints of the ligand. The trans angles at ruthenium fall in the range 177.11 (8)-179.32 (8)°, while the cis angles range from 86.49 (8) to 93.45 (8)°. The Ru-N bond lengths of 2.006 (2)-2.028 (2) Å are short and reflect the π-acceptor character of the pyrazole ligand. It is noteworthy that the average value of 2.014 (2) Å is similar to the value of 2.013 (2) Å found in $[Ru(bpy)_2(Cl)_2]$[16] for the Ru-N(bpy) bonds that are trans to the chloride ligand but much shorter than the value of 2.054 (2) Å observed in the same structure for Ru-N(bpy) bonds that are trans to the second N atom of the bpy ligand. The Ru-O(water) distances ranges from 2.121 (2) to 2.139 (2) Å, which is consistent with the values of 2.107 (2)-2.139 (2) Å observed in the hexaaquaruthenium(II) cation.[17]

The ligand consists of three entirely planar pyrazole groups bound to the central carbon atom C(1); this atom lies in the plane of the A ring but is slightly out of the plane of the B [0.025 (4) Å] and C [0.040 (4) Å] rings. The three pyrazole rings are mutually inclined at roughly 60°, the observed values being 62, 63, and 55°.

The *p*-toluenesulfonate anions are unremarkable, consisting of planar six-member rings coordinated to approximately tetrahedral

Table IV. Bond Angles (deg) in [(tpm)Ru(H2O)3](p-CH3C6H4SO3)2·1.5H2O

N(2A)-Ru-N(2B)	86.49 (8)	N(1C)-N(2C)-C(3C)	104.7 (2)
N(2A)-Ru-N(2C)	87.46 (8)	N(2C)-C(3C)-C(4C)	110.7 (2)
N(2A)-Ru-O(1)	179.32 (8)		
N(2A)-Ru-O(2)	91.11 (7)	C(3C)-C(4C)-C(5C)	106.4 (2)
N(2A)-Ru-O(3)	89.61 (7)	N(1C)-C(5C)-C(4C)	106.8 (2)
N(2B)-Ru-N(2C)	87.09 (9)		
N(2B)-Ru-O(1)	93.07 (8)	O(11)-S(1)-O(12)	110.0 (2)
N(2B)-Ru-O(2)	177.11 (8)	O(11)-S(1)-O(13)	111.9 (2)
N(2B)-Ru-O(3)	93.45 (8)	O(11)-S(1)-C(1P1)	107.4 (1)
N(2C)-Ru-O(1)	93.04 (9)	O(12)-S(1)-O(13)	113.0 (2)
N(2C)-Ru-O(2)	91.19 (8)	O(12)-S(1)-C(1P1)	107.0 (1)
N(2C)-Ru-O(3)	176.99 (8)	O(13)-S(1)-C(1P1)	107.2 (1)
O(1)-Ru-O(2)	89.34 (7)	O(21)-S(2)-O(22)	111.2 (1)
O(1)-Ru-O(3)	89.89 (8)	O(21)-S(2)-O(23)	112.0 (1)
O(2)-Ru-O(3)	88.15 (7)	O(21)-S(2)-C(1P2)	106.2 (1)
N(1A)-C(1)-N(1B)	109.6 (2)	O(22)-S(2)-O(23)	113.4 (1)
N(1A)-C(1)-N(1C)	110.3 (2)	O(22)-S(2)-C(1P2)	105.9 (1)
N(1B)-C(1)-N(1C)	110.6 (2)	O(23)-S(2)-C(1P2)	107.5 (1)
C(1)-N(1A)-N(2A)	117.5 (1)	S(1)-C(1P1)-C(2P1)	120.2 (2)
C(1)-N(1A)-C(5A)	130.5 (2)	S(1)-C(1P1)-C(6P1)	120.3 (2)
N(2A)-N(1A)-C(5A)	112.0 (1)	C(2P1)-C(1P1)-C(6P1)	119.5 (2)
Ru-N(2A)-N(1A)	118.7 (1)	C(1P1)-C(2P1)-C(3P1)	119.8 (2)
Ru-N(2A)-C(3A)	136.9 (1)	C(2P1)-C(3P1)-C(4P1)	121.3 (2)
N(1A)-N(2A)-C(3A)	104.5 (1)	C(3P1)-C(4P1)-C(5P1)	118.2 (2)
N(2A)-C(3A)-C(4A)	110.8 (2)	C(3P1)-C(4P1)-C(7P1)	121.4 (3)
C(3A)-C(4A)-C(5A)	106.4 (2)	C(5P1)-C(4P1)-C(7P1)	120.4 (3)
N(1A)-C(5A)-C(4A)	106.3 (2)	C(4P1)-C(5P1)-C(6P1)	121.1 (2)
C(1)-N(1B)-N(2B)	119.4 (2)	C(1P1)-C(6P1)-C(5P1)	120.0 (2)
C(1)-N(1B)-C(5B)	129.6 (2)	S(2)-C(1P2)-C(2P2)	120.7 (2)
N(2B)-N(1B)-C(5B)	110.9 (2)	S(2)-C(1P2)-C(6P2)	119.4 (2)
Ru-N(2B)-N(1B)	116.4 (1)	C(2P2)-C(1P2)-C(6P2)	119.9 (3)
Ru-N(2B)-C(3B)	138.2 (1)	C(1P2)-C(2P2)-C(3P2)	119.9 (3)
N(1B)-N(2B)-C(3B)	105.4 (2)	C(2P2)-C(3P2)-C(4P2)	121.6 (3)
N(2B)-C(3B)-C(4B)	110.5 (2)	C(3P2)-C(4P2)-C(5P2)	117.2 (3)
C(3B)-C(4B)-C(5B)	106.7 (2)	C(3P2)-C(4P2)-C(7P2)	121.3 (3)
N(1B)-C(5B)-C(4B)	106.4 (2)	C(5P2)-C(4P2)-C(7P2)	121.5 (3)
C(1)-N(1C)-N(2C)	119.0 (2)	C(4P2)-C(5P2)-C(6P2)	121.8 (3)
C(1)-N(1C)-C(5C)	129.7 (2)	C(1P2)-C(6P2)-C(5P2)	119.6 (3)
N(2C)-N(1C)-C(5C)	111.3 (2)		
Ru-N(2C)-N(1C)	117.3 (1)		
Ru-N(2C)-C(3C)	137.8 (2)		

(15) (a) Boggess, R. K.; Zatko, D. A. *Inorg. Chem.* **1976**, *15*, 626. (b) Canty, A. J.; Minchin, N. J. *J. Organomet. Chem.* **1982**, *226*, C14. (c) Canty, A. J.; Minchin, N. J.; Healy, P. C.; White, A. H. *J. Chem. Sooc., Dalton Trans.* **1982**, 1795. (d) Szalda, D.; Keene, F. R. *Inorg. Chem.* **1986**, *25*, 2795. (e) Keene, F. R.; Snow, M. R.; Stephenson, P. J.; Tiekink, E. R. T. *Inorg. Chem.* **1988**, *27*, 2040.

(16) Eggleston, D. S.; Goldsby, K. A.; Hodgson, D. J.; Meyer, T. J. *Inorg. Chem.* **1985**, *24*, 4573.

(17) Bernhard, P.; Burgi, H.; Hauser, J.; Lehmann, H.; Ludi, A. *Inorg. Chem.* **1982**, *21*, 3936.

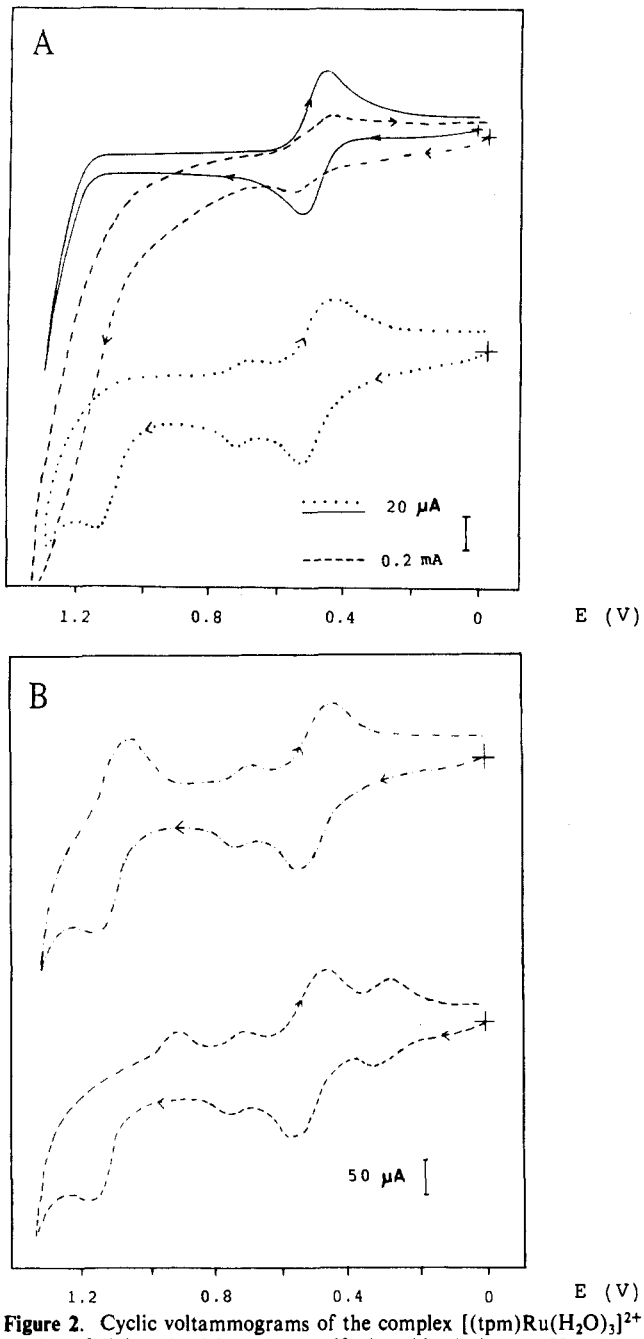

Figure 2. Cyclic voltammograms of the complex $[(tpm)Ru(H_2O)_3]^{2+}$ (cation of **1**) in a 0.1 M *p*-toluenesulfonic acid solution at pH = 1 (vs SSCE), scan rate 100 mV/s: (A) unactivated glassy-carbon electrode (—), activated glassy-carbon electrode (···), addition of benzyl alcohol (0.045 mM) to the former solution at an activated glassy-carbon electrode (- - -); (B) as in (A), but at a scan rate of 2 V/s at an activated glassy-carbon electrode (- - -) and a scan obtained after holding the potential at 1.25 V for 30 s (- - -) both at an activated electrode.

sulfur atoms; the bond angles at sulfur fall in the range 105.9 (1)–113.4 (1)°, the S–O bond lengths lie between 1.387 (2) and 1.459 (2) Å.

There is extensive hydrogen bonding in the crystals with all three of the coordinated water molecules [O(1), O(2), and O(3)] on the complex cation donating two hydrogen bonds to oxygen atoms of the anion or the O atoms of solvent molecules. The metrical parameters associated with these and other hydrogen bonds are presented in Table V.

Redox Chemistry. The electrochemistry of the triaqua monomer **1** in aqueous solution provides evidence for the presence of several pH-dependent oxidative processes within the limits of the solvent. Cyclic voltammograms of **1** in a 0.1 M *p*-toluenesulfonic acid solution as obtained at a normal glassy-carbon electrode are shown in Figure 2A. In the same figure is shown the impact on the voltammetry of electrode activation, as well as the catalytic effect

Table V. Hydrogen-Bond Parameters in $[(tpm)Ru(H_2O)_3](p\text{-}CH_3C_6H_4SO_3)_2 \cdot 1.5H_2O$

A–H···B	A···B, Å	A–H···B, deg	symmetry of B
O(1)–H(O1A)···O(12)	2.664 (3)	154	$-x, -y, 1-z$
O(1)–H(O1B)···O(13)	2.932 (4)	136	$x, y, z-1$
O(2)–H(O2A)···OW(1)	2.746 (3)	173	$x, y, z-1$
O(2)–H(O2B)···O(13)	2.750 (3)	159	$x, y, z-1$
O(3)–H(O3A)···OW(1)	2.802 (2)	162	$-x, 1-y, 1-z$
O(3)–H(O3B)···O(22)	2.673 (3)	168	$-x, 1-y, 1-z$
OW(1)–H(W1A)···O(21)	2.690 (3)	176	x, y, z

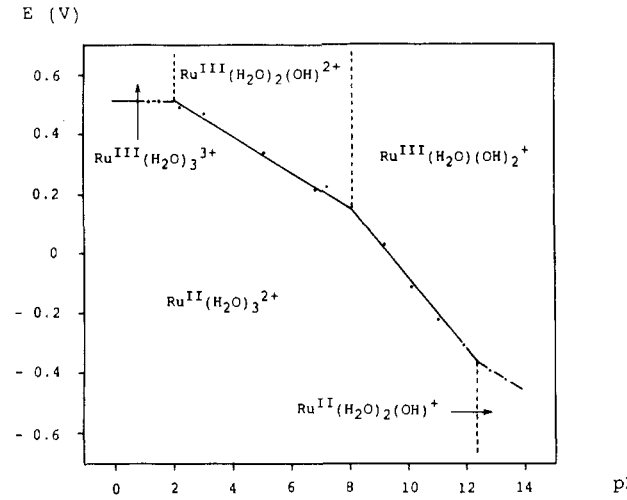

Figure 3. Plot of $E_{1/2}$ vs pH for the reversible Ru(III/II) couple for $[(tpm)Ru(H_2O)_3]^{2+}$. The dominant forms of the couple with regard to oxidation state and proton composition are indicated on the diagram by using abbreviations such as $Ru^{III}(H_2O)_2(OH)^{2+}$ for $[(tpm)Ru^{III}(H_2O)_2(OH)]^{2+}$. The pK_a values for the two oxidation states are shown as the vertical dashed lines.

of added benzyl alcohol on the electrode response. In Figure 2B is shown the result of increasing the scan rate to 2 V/s. Evidence of oxidative decomposition was obtained by holding the potential at 1.25 V for 30 s, as shown by the appearance of the new waves in the cyclic voltammogram in Figure 2B. In the cyclic voltammogram of **1** at pH 1.0 in a 0.1 M *p*-toluenesulfonic acid solution (Figure 2A), a one-electron reversible wave appears at $E_{1/2} = 0.51$ V ($E_{p,a} - E_{p,c} = 60$ mV at a scan rate of 100 mV/s) for the expected Ru(III)/Ru(II) couple. Coulometric oxidation of **1** at $E_{app} = 0.6$ V occurs with $n = 0.9$ to give the Ru(III) analogue, corroborating the one-electron nature of the process.

pH Dependence of the Ru(III)/Ru(III) Couple. The pH dependence of the III/II couple for the triaqua monomer **1** is shown in Figure 3. The experimental data were obtained from pH-dependent cyclic voltammetric measurements. In the diagram the dominant form of the couple with regard to oxidation state and proton composition in the various pH–potential regions is indicated. In the labeling scheme abbreviations such as $Ru^{III}(H_2O)_2(OH)^{2+}$ are used, for example, for $[(tpm)Ru^{III}(H_2O)_2(OH)]^{2+}$. The proton compositions of the complexes were inferred by comparing the slopes of the $E_{1/2}$ vs pH lines to values calculated from the Nernst equation: $E_{1/2} = E_{1/2}° - (0.059m/n)$pH, where $E_{1/2}°$ is the half-wave potential at pH = 0 and m is the number of protons gained when n electrons are gained. The pK_a values were taken as the breaks in the $E_{1/2}$–pH lines and are shown as the vertical dashed lines. In terms of proton content, the couple varies from eq 6 at pH < 2.1 to eq 7 at pH > 12.3. In Table

$$[(tpm)Ru^{III}(H_2O)_3]^{3+} + e \rightarrow [(tpm)Ru^{II}(H_2O)_3]^{2+} \quad (6)$$

$$[(tpm)Ru^{III}(H_2O)(OH)_2]^{+} + e + H^{+} \rightarrow [(tpm)Ru^{II}(H_2O)_2(OH)]^{+} \quad (7)$$

VI are listed pK_a and $E_{1/2}$ values at 23 °C vs SSCE ($\mu = 0.1$ M; pH = 1) for the $[(tpm)Ru^{II}(H_2O)_3]^{2+}$-based Ru(III/II) couple and for several aqua–polypyridyl complexes for purposes of comparison.

Table VI. pK_a and $E_{1/2}$ Values (vs SSCE at pH = 1) at 23 °C (μ = 0.1 M)

complex	Ru(II)		Ru(III)		$E_{1/2}$, V		
	pK_{a1}	pK_{a2}	pK_{a1}	pK_{a2}	Ru(III/II)	Ru(IV/III)	Ru(IV/V)
$[(tpm)(bpy)Ru(H_2O)]^{n+}$ [a]	10.8		1.9		0.70	1.25	
cis-$[(bpy)_2Ru(H_2O)_2]^{n+}$ [b]	8.9		1.5	5.2	0.63	0.94	1.10
trans-$[(bpy)_2Ru(H_2O)_2]^{n+}$ [b]	9.2	>11.5	<1	5.2	0.47	0.85	1.05[d]
$[(tpm)Ru(H_2O)_3]^{n+}$ [c]	12.2		2.1	8.0	0.51	0.71	1.19[e]

[a] Reference 12b. [b] Reference 8f. [c] This work. [d] This is the $E_{1/2}$ value for the Ru(VI/IV) couple. [e] This value corresponds to the oxidative peak potential for the wave. The couple is irreversible.

Higher Oxidation State Couples. A second wave appears at $E_{1/2}$ = 0.68 V at pH = 1 in a 0.1 M *p*-toluenesulfonic acid solution for the triaqua complex **1** at an activated electrode. As shown by chemical oxidation by Ce(IV), the redox process that occurs at this wave is a 1e process corresponding to oxidation of Ru(III) to Ru(IV). Although the wave appears to be reversible, it is kinetically slow as shown by the diminished peak heights of the anodic and cathodic peak currents compared to those of the Ru(III)/(II) couple. Because of slow oxidation at the electrode, oxidation by Ce(IV) was the preferred method of generating Ru(IV).

The same effect has been observed for the Ru(IV)/(III) and Ru(III)/(II) couples of $[(bpy)_2(py)Ru(H_2O)]^{2+}$. The direct oxidation of Ru(III) to Ru(IV) at the electrode is slow because either initial oxidation by electron transfer, $Ru^{III}(OH)^{2+} \rightarrow Ru^{IV}(OH)^{3+}$, followed by proton loss, or initial proton loss, $Ru^{III}(OH)^{2+} \rightarrow Ru^{III}(O)^{+}$, followed by oxidation, involves high-energy intermediates. This causes slow electron transfer at the electrode.[6d,s]

At pH 1.0, and a scan rate of 100 mV/s, a third oxidative wave is observed at $E_{p,a}$ = 1.19 V but only at acvtivated electrodes. The wave is chemically irreversible at 100 mV/s, as shown by the absence of a reductive, return component. Because of the chemical instability of the oxidized form of this couple, it was not possible to determine *n* by coulometry. However, a comparison of peak currents between this wave and the oxidative component of the Ru(III/II) wave suggests that it arises from a one-electron couple and further oxidation of Ru(IV) to Ru(V). From the data in Table VI, $E_{1/2}$ values for Ru(IV)/Ru(III) and Ru(V)/Ru(IV) couples based on *cis*-$[(bpy)_2Ru(H_2O)_2]^{2+}$ occur at 0.94 and 1.10 V under the same conditions.

As shown in Figure 2B, when the scan rate of the cyclic voltammetry is increased to 2 V/s, the Ru(V)/Ru(IV) couple becomes reversible. The implied scan rate dependence shows that following oxidation of Ru(IV) to Ru(V) an irreversible chemical step occurs on a time scale of seconds. The consequences of the decomposition chemistry are also illustrated in Figure 2B by the response after the potential of the electrode was held at 1.25 V for 30 s during an oxidative scan. New waves appear at $E_{p,c}$ = 0.75 and $E_{1/2}$ = 0.32 V on a reductive scan following the potential hold. The same results were obtained by cyclic voltammetry when more than 2 equiv of Ce(IV) was added to the initial solution at pH = 1.0. The wave at $E_{1/2}$ = 0.32 V is a reversible process with a peak splitting of $\Delta E_p = E_{p,c} - E_{p,a}$ = 65 mV. The instability at Ru(V) is a property shared with $[(trpy)(bpy)Os^{II}(H_2O)]^{2+}$ (trpy is 2,2′:6′,2″-terpyridine) and *cis*-$[(bpy)_2Ru(H_2O)_2]^{2+}$.[6j,8f] In those cases the instability arises by ligand loss, disproportionation and concomitant formation of *trans*-dioxo M(VI) products.

The driving force for ligand loss appears to be the electronic stabilization associated with the formation of the d^2 *trans*-dioxo group. For the tpm complex, oxidation to Ru(V) is presumably followed by disproportionation, $2Ru(V) \rightarrow Ru(VI) + Ru(IV)$, and the opening of the chelating framework of the tpm ligand. This would give the analogue of *trans,cis*-$[(bpy)Ru^{VI}(O)_2(OH)_2]$ with one of the pyrazolyl groups protonated, $[(tpmH)Ru^{VI}(O)_2(OH)_2]^{+}$. The appearance of the reversible wave at $E_{1/2}$ = 0.32 V for the decomposition product is consistent with a Ru(III)/Ru(II) couple in which a moderately back-bonding pyrazole group is replaced by H_2O or OH^-.[2f]

The retention of the tpm ligand is suggested by the following experiment. Oxidation of $[(tpm)Ru(H_2O)_3]^{2+}$ in 0.1 M *p*-$CH_3C_6H_4SO_3H$ by the 3 equiv of Ce(IV) followed by Zn(Hg) reduction gave $[(tpm)Ru(H_2O)_3]^{2+}$, as shown by the reappearance of its characteristic cyclic voltammogram. Apparently, upon reduction of Ru(VI) to Ru(II) the electronically based structural demands of the *trans*-dioxo group are lost and the third arm of the chelate recloses.

The point that stands out in this and the earlier work is the difficulty of stabilizing the d^2 *cis*-dioxo structure. A strong thermodynamic driving force for cis → trans isomerization clearly exists and facile kinetic pathways are available in water, which allow the isomerization to occur.[8a,f,18] Clearly, unusual strategies will have to be adopted in order to have access to the more reactive *cis*-dioxo coordination geometry.

In acidic solutions under aerobic conditions the triaqua complex **1** is stable for days. However, in neutral or basic solutions an O_2-induced coupling occurs to give, what is presumably, a (μ-oxo)tetraaquaruthenium complex (reaction 8). The μ-oxo com-

$$2[(tpm)Ru(H_2O)_3]^{2+} + \tfrac{1}{2}O_2 \rightarrow [(tpm)(H_2O)_2Ru^{III}\text{–}O\text{–}Ru^{III}(H_2O)_2(tpm)]^{4+} + 2H_2O \quad (8)$$

plex has an intense low-energy absorption band (at λ_{max} = 570 nm) that is a characteristic feature of the M(III)–O–M(III) μ-oxo link in structures of this kind.[12d] The characterization and redox properties of the μ-oxo complex are currently under investigation.

In the presence of benzyl alcohol (0.045 mM), the III/II wave appears, but with enhanced current, and the onset of a small catalytic oxidation wave appears just past the IV/III wave. There is a considerable current enhancement at the onset of the V/IV wave. An appreciable fraction of the current at and past 1.2 V comes from direct oxidation of benzyl alcohol at the electrode. Rate and mechanistic details for the oxidation of benzyl alcohol by $[(bpy)_2(py)Ru^{IV}(O)]^{2+}$ and *trans*-$[(TMC)(X)Ru^{V}(O)]^{2+}$ (TMC = 1,4,8,11-tetramethyl-1,4,8,11-tetraazacyclotetradecane; X = Cl, NCO, N_3) have been reported.[6r,7e] The current enhancements at low and high potentials may be attributable to Ru(IV), presumably as $[(tpm)Ru^{IV}(O)(H_2O)_2]^{2+}$, and to Ru(V), as $[(tpm)Ru^{V}(O)_2(H_2O)]^{+}$, respectively, although the existence of the apparent overvoltages are not understood. The implied rate of oxidation of benzyl alcohol is impressive and suggests that even given the decomposition chemistry, the tpm-based aqua complex is capable of acting as an electrocatalyst toward reactive substrates. The rate of oxidation of benzyl alcohol is more rapid than the rate of decomposition of Ru(V). If the rate of oxidation of benzyl alcohol by Ru(V) is first order in both Ru(V) and in the alcohol, as it is for $[(bpy)_2(py)Ru^{IV}(O)]^{2+}$, $k > 20\ M^{-1}\ s^{-1}$.

Spectral Properties. UV–visible spectral changes associated with the different oxidation states beginning with $[(tpm)Ru(H_2O)_3]^{2+}$ at pH = 1 in a 0.1 M *p*-toluenesulfonic acid are shown in Figure 4. For $[(tpm)Ru(H_2O)_3]^{2+}$, two bands of nearly equal intensity appear at 290 (ϵ = 6680) and 326 nm (ϵ = 6530 $M^{-1}\ cm^{-1}$). The higher energy band is a tpm-localized $\pi \rightarrow \pi^*$ transition, and the second, a $d\pi(Ru(II)) \rightarrow \pi^*(tpm)$ metal to ligand charge-transfer transition.[12b] Following electrochemical oxidation of Ru(II) to Ru(III) a new band appears at 340 nm (ϵ = 2190) which is probably a tpm → Ru(III) charge-transfer transition. Upon oxidation, the $\pi \rightarrow \pi^*$ band increases in energy and appears at 260 nm (ϵ = 6870). In the absorption spectrum

(18) Durham, B.; Wilson, S. R.; Hodgson, D. J.; Meyer, T. J. *J. Am. Chem. Soc.* **1980**, *102*, 600.

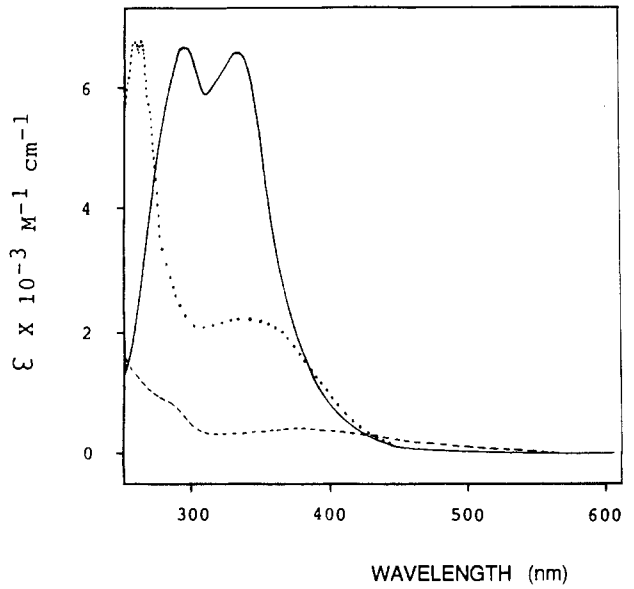

Figure 4. Uv-visible spectra at pH = 1 of $[(tpm)Ru^{II}(H_2O)_3]^{2+}$ (—), of electrochemically generated $[(tpm)Ru^{III}(H_2O)_3]^{3+}$ (n = 0.9) (···), and of $[(tpm)Ru^{IV}(O)(H_2O)_2]^{2+}$ (---) generated by adding 2 equiv of Ce(IV) to $[(tpm)Ru^{II}(H_2O)_3]^{2+}$.

of the Ru(IV) complex, generated chemically by adding 2 equiv of Ce(IV) to $[(tpm)Ru^{II}(H_2O)_3]^{2+}$, an absorption band of low intensity appears at 374 nm (ϵ = 408). The $\pi \rightarrow \pi^*$(tpm) transition is further shifted to higher energy and is not shown in the spectrum.

The ^{1}H NMR spectrum of the triaquaruthenium complex **1** in D_2O was assigned[19] (the assignments are listed in the Experimental Section) by taking advantage of the symmetry of the molecule. The three pyrazolyl rings of the tpm ligand are equivalent, which greatly simplifies integrations. The methylenic proton of the tpm ligand is not observed in the spectrum due to a fast-exchange process with D_2O. In 0.1 M DCl a new resonance appears at 9.2 ppm (s, 1), which can be assigned to this proton. This resonance does not appear in 0.1 M NaOD. From the absence of shifts in the remaining resonances, it can be inferred that anation by Cl^- is relatively unimportant under these conditions.

Acknowledgments are made to the National Science Foundation under Grant No. CHE-8601604 and the National Institutes of Health under Grant No. GM32296 for support of this research. A.L. acknowledges support from a Fulbright "La Caixa" Fellowship (Barcelona, Spain).

Registry No. **1**, 128824-20-4; **2**, 128824-24-8; $[(tpm)Ru(H_2O)_3]^{3+}$, 128824-21-5; $[(tpm)Ru(H_2O)_3]^{4+}$, 128824-22-6; $[(tpm)Ru(H_2O)_3]^{5+}$, 128824-23-7.

Supplementary Material Available: Listings of hydrogen atom positions and anisotropic thermal parameters (4 pages); a table of observed and calculated structure amplitudes (24 pages). Ordering information is given on any current masthead page.

(19) Pretsch, E.; et al. *Tables of Spectral Data for Structure Determination of Organic Compounds*; Springer-Verlag: West Berlin, 1983.

Contribution from the Chemistry Department,
The Ohio State University, Columbus, Ohio 43210

Inclusion Complex Formation Involving a New Class of Transition-Metal Host

Thomas J. Meade, Nathaniel W. Alcock, and Daryle H. Busch*

Received November 7, 1989

This new class of transition-metal-containing host molecule readily accommodates aromatic rings as guests. The complexation is regiospecific and driven by hydrophobic interactions in aqueous media. Crystallographic data have confirmed the expanded cavity size and the nature of the new hosts. An experimentally justified NMR relaxation technique provided structural information about the guest-host complex in solution. Crystal data for the supervaulted host $[Ni\{Me_2(bipiperidiniumyl)_2$-9,10-anthra[16]-cyclidene$\}](PF_6)_2$: space group $P2_1/c$, a = 14.172 (4) Å, b = 16.235 (5) Å, c = 34.705 (10) Å, β = 109.76°, Z = 4, R = 0.112 for 1775 observed reflections.

Introduction

The field of host-guest chemistry continues to enjoy increasing importance as a vehicle for the study of catalysis, enzyme modeling, and facilitated transport. Several intensively studied classes of hosts, including cyclodextrins, cavitands, and cryptates,[1] form inclusion complexes characterized by the absence of covalent bond formation.[2] Enzymes such as cytochrome P-450[2] exploit hydrophobic interactions as the driving force for enzyme-substrate binding,[3,4] and it is on these interactions that this work and previous work in our laboratory have focused.

The development by Takeuchi of the macrobicyclic ligands known as vaulted cyclidenes led to a credible model of the ternary complex of cytochrome P-450[5-7] (Figure 1). The metal cyclidene hosts bind small organic molecules regiospecifically,[8,9] while simultaneously providing a vacant coordination site on the metal atom for the coordination of dioxygen. Previous NMR chemical shift studies on aqueous solutions first demonstrated host-guest association[5-7] by these transition metal complexes. The copper(II)

* To whom correspondence should be addressed at the Department of Chemistry, University of Kansas, Lawrence, KS 66045-0046.

(1) For reviews, see: (a) Szejtli, J. *Cyclodextrins and Their Inclusion Complexes*; Akademiai Kiado: Budapest, 1982; 296 pp. (b) Tabushi, I. *Tetrahedron* **1984**, *40*, 269. (c) Rossa, L.; Vogtle, F. *Topics in Current Chem.* **1983**, *113*, 1. (d) Cram, D. J. *Science* **1983**, *219*, 1177. Meade, T. J.; Busch, D. H. *Prog. Inorg. Chem.* **1985**, *33*, 59.
(2) Sato, R.; Omura, T. *Cytochrome P-450*; Academic Press: New York, 1978.
(3) (a) White, R. E.; Coon, M. J. *Annu. Rev. Biochem.* **1980**, *49*, 314. (b) White, R. E.; Oprian, D. D.; Coon, M. J. In *Microcomes, Drug Oxidations, and Chemical Carcinogenesis*; Coon, M. J., Connery, A. H., Estabrook, R. W., Gelboin, H., Gillette, J. R., O'Brien, P. J., Eds.; Academic Press: New York, 1980; p 243.
(4) Poulos, T. L.; Finzel, B. C.; Gunsalus, I. C.; Wagner, G. C.; Kraut, J. *J. Biol. Chem.* **1985**, *25*, 16122.
(5) Takeuchi, K. J.; Busch, D. H.; Alcock, N. J. *J. Am. Chem. Soc.* **1981**, *103*, 2421.
(6) Takeuchi, K. J.; Busch, D. H.; Alcock, N. J. *J. Am. Chem. Soc.* **1983**, *105*, 4261.
(7) Takeuchi, K. J.; Busch, D. H. *J. Am. Chem. Soc.* **1983**, *105*, 6812.
(8) Kwik, W.-L.; Herron, N.; Takeuchi, K.; Busch, D. H. *J. Chem. Soc., Chem. Commun.* **1983**, 409.

0020-1669/90/1329-3766$02.50/0